Measurements of Long-Range Interactions between Protein-Functionalized Surfaces by Total Internal Reflection Microscopy

ARTICLE *in* LANGMUIR · FEBRUARY 2015

Impact Factor: 4.46 · DOI: 10.1021/acs.langmuir.5b00090 · Source: PubMed

3 AUTHORS, INCLUDING:

Xiangjun Gong

South China University of Technology

13 PUBLICATIONS **72** CITATIONS

SEE PROFILE

To Ngai

The Chinese University of Hong Kong

94 PUBLICATIONS **1,304** CITATIONS

SEE PROFILE

Langmuir

Article

pubs.acs.org/Langmuir

Measurements of Long-Range Interactions between Protein-Functionalized Surfaces by Total Internal Reflection Microscopy

Zhaohui Wang,[†] Xiangjun Gong,*[,‡] and To Ngai*[,†]

[†]Department of Chemistry, The Chinese University of Hong Kong, Shatin, N.T., Hong Kong

[‡]School of Materials Science and Engineering, South China University of Technology, Guangzhou, China 510640

ABSTRACT: Understanding the interaction between protein-functionalized surfaces is an important subject in a variety of protein-related processes, ranging from coatings for biomedical implants to targeted drug carriers and biosensors. In this work, utilizing a total internal reflection microscope (TIRM), we have directly measured the interactions between micron-sized particles decorated with three types of common proteins concanavalin A (ConA), bovine serum albumin (BSA), lysozyme (LYZ), and glass surface coated with soy proteins (SP). Our results show that the protein adsorption greatly affects the charge property of the surfaces, and the interactions between those protein-functionalized surfaces depend on solution pH values. At pH 7.5−10.0, all these three protein-functionalized particles are highly negatively charged, and they move freely above the negatively charged SP-functionalized surface. The net interaction between protein-functionalized surfaces captured by TIRM was found as a long-range, nonspecific double-layer repulsion. When pH was decreased to 5.0, both protein-functionalized surfaces became neutral and double-layer repulsion was greatly reduced, resulting in adhesion of all three protein-functionalized particles to the SP-functionalized surface due to the hydrophobic attraction. The situation is very different at pH = 4.0: BSA-decorated particles, which are highly charged, can move freely above the SP-functionalized surfaces, while ConA- and LYZ-decorated particles can only move restrictively in a limited range. Our results quantify these nonspecific *kT*-scale interactions between protein-functionalized surfaces, which will enable the design of surfaces for use in biomedical applications and study of biomolecular interactions.

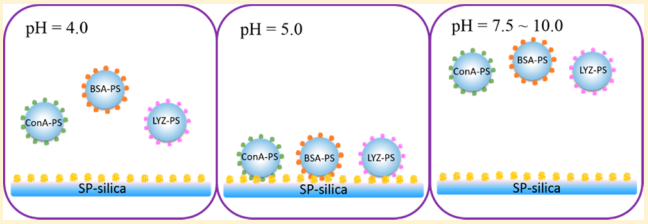

INTRODUCTION

In a biological system like cells, proteins located on the interfaces keep interacting with many types of molecules and components to maintain life activities.[1] These proteins on surfaces play important roles in controlling the structure and function of specific biological systems and thus are the most important components for biointerfaces.[2] However, if the proteins are inadvertently adsorbed to the surface, the deposition of bacteria, cells, or other microorganisms may occur,[3] which in turn can cause severe problems in real applications such as biosensors, water purification, and ship shells.[4] Therefore, understanding the mechanism of protein adsorption on surfaces as well as interactions between protein-functionalized surfaces[5] is an important subject for guidance to design specific biointerfaces for inhibiting or reducing non-specific protein adsorption[6] in a variety of biological-related processes and applications.

In the past two decades, many types of surfaces functionalized with hydrophilic polymers including polysaccharides,[7,8] phospholipids,[9] zwitterionic polymers,[10,11] poly(ethylene glycol) (PEG),[12,13] and other materials have been developed to control protein adsorption and cellular adhesion. For example, Chien et al. showed that surfaces coated with zwitterionic polymers could significantly reduce protein adsorption and attachment of L929 cells and platelets.[11] Meanwhile, Zhang et al. reported that surfaces grafted with PEG chains were highly resistant to both protein adsorption and cell attachments even in blood plasma.[13] Among the protein-resistant materials described above, protein molecules, which are composed of amino acids, can also be considered as one kind of zwitterionic polymers and thus are expected to be a potential candidate for preparing protein resistant and antimicrobial surfaces. It was reported that protein mixtures extracted from fish,[14] hydrophobin,[15] and soy protein isolate[3] could decrease protein adsorption, and the involved interaction was pH-dependent. The related interactions have been investigated by traditional methods such as quartz crystal microbalance (QCM) and isothermal titration calorimetry (ITC),[3,15] but these methods are unable to give quantitative results as well as provide the origin of the interactions.

In recent years, another emerging alternative technique, total internal reflection microscopy (TIRM), has been applied for directly measuring interactions between protein- and polymer-functionalized surfaces.[16] By noninvasively monitoring the diffusing colloids interacting with a surface decorated with specific proteins, this technique exploits natural gauges for energy (kT) and height (nm) when interrogating protein−protein interactions. While TIRM has been employed in a few

Received: January 9, 2015
Revised: February 26, 2015
Published: February 26, 2015

DOI: 10.1021/acs.langmuir.5b00090
Langmuir 2015, 31, 3101−3107

experiments to capture the interactions between lipid-functionalized surfaces, protein, and carbohydrate-functionalized surfaces,[17,18] the nonspecific interactions between several typical protein-functionalized surfaces are rarely reported in a systematic manner. For example, soy protein is a kind of protein that is environmentally friendly and abundant,[19] making it a suitable candidate for developing protein-resistant surface.

In this work, we use TIRM to directly monitor the interaction between glass surfaces decorated with soy protein (SP) and Brownian colloids coated with three types of common proteins: Concanavalin A (ConA, a lectin extracted from Jack Bean, which can specifically bind to α-mannose and glucose), bovine serum albumin (BSA, a serum globulin protein derived from cows and the main component in blood), and lysozyme (LYZ, glycoside hydrolases).[20,21] kT- and nanometer-scale interactions between these two surfaces functionalized with different proteins were obtained. Besides, a series of zeta-potential experiments were conducted to provide complementary information about the electric properties of these protein-functionalized surfaces at various pH values. A combination of electrophoresis and TIRM measurement illustrates that the interactions between SP and ConA/BSA/LYZ protein-functionalized surfaces is pH dependent and mainly governed by electrostatic repulsion and hydrophobic attraction. The obtained information on interactions and mechanisms involving protein-functionalized surfaces will help us to further quantify specific interactions in integrated synthetic-biomolecular materials, devices, and systems.

MATERIALS AND METHODS

Materials. Soy protein (SP) with a protein content of minimum 90% (on dry basis) was obtained from Linyi Shansong Biological Products Co., China. Lysozyme (LYZ) from chicken egg white (M_w = 14.7 kDa), Concanavalin A (ConA) from *Canavalia ensiformis* (M_w = 104−112 kDa), and BSA (M_w = 68 kDa) from Sigma-Aldrich Co. were used as received. Dichlorodimethylsilane (99%) was purchased from Acros Organics and used without further purification. Polystyrene (PS) latexes with a diameter of ∼5.6 μm (CV 4.1%) were purchased from Life Technologies Corp., while silica particles with a diameter of 5 μm (CV 10.0%) and PS latexes with a diameter of 100 nm (CV 2.6%) were purchased from Polysciences Inc. Glass slides (BK-7) were purchased from Fischer Scientific Co. Silicon wafers (single side polished), ⟨111⟩, N-type, diameter × thickness 5 in. × 0.5 mm, were purchased from Zhejiang Lijing Silicon Materials Co., China.

Sample Preparation. *Soy Protein (SP)-Functionalized Glass Slides and Silica Particles.* Glass slides were first immersed in piranha solution (H_2SO_4 (98% v/v):H_2O_2 (30% v/v) = 3:1) overnight and cleaned by repeatedly rinsing with deionized water (DI water). We treated slides further by cleaning them with an ultraviolet (UV)-ozone plasma cleaner (Harrick Sci. Corp.). The cleaned slides were then modified to become hydrophobic with 1% (v/v) dichlorodimethylsilane in toluene for 1 h. After rinsed thoroughly with toluene, chloroform, and acetone, they were dried with nitrogen gas. For adsorption of SP, 1.0% (w/w) SP was first dissolved in DI water at 70 °C for ensuring complete dissolution, and then the slides were immersed in the solution for 12 h.[19] After that, they were rinsed with DI water thoroughly to remove excess protein molecules.

To obtain the electric properties of the glass slide after adsorption of proteins, silica particles (diameter = 5.0 μm) adsorbed with SP were used for zeta-potential measurement because they have similar surface properties as the glass slides. Before the measurements, the SP-adsorbed silica particles were purified by centrifugation for three times. A mixture of sodium chloride (NaCl), hydrocholoric acid (HCl), and sodium hydroxide (NaOH) with a similar ionic strength but different pH values were used to dilute the SP-coated silica particles for the measurements. On the other hand, in order to see whether the adsorbed SP layers will be washed off at different pH values, the SP-coated silica particles were washed separately with 0.1 mM NaCl, 0.1 mM HCl, and 0.1 mM NaOH and then centrifuged four times.

Adsorption of Three Common Proteins (ConA, BSA, and LYZ) on PS Particles. We prepared all the protein-functionalized surfaces at a relatively high ionic strength solution to minimize the effect induced by differences of electric properties.[22] For ConA, BSA, and LYZ, 10 mM PBS buffer (pH = 7.4) was used as the solvent. After that, 50 μL of PS latexes at two different diameters (5.6 μm for TIRM and 100 nm for dynamic light scattering measurements) were diluted to 1 mL by PBS solution containing ConA/BSA/LYZ of 10 mg/mL, which is in excess amount to fully cover the surfaces. After shaking overnight, they were purified by centrifugation for three times and termed as ConA-PS, BSA-PS, and LYZ-PS in the following discussion.

Characterization. *Size of PS Particles before and after Protein Adsorption As Measured by Dynamic Light Scattering (DLS).* The change of the average hydrodynamic radius ($\langle R_h \rangle$) of the 100 nm PS latexes after protein adsorption was determined by a portable dynamic light scattering instrument (Portable Particle Sizer, JiankeInstru., China). The particles before and after protein (ConA/BSA/LYZ) adsorption were first purified to remove excess proteins, filtered through a filter membrane with 0.5 μm diameter, and then measured at 30° for 900 s. The correlation functions were then analyzed by cumulant fit to yield a final size.

Thickness of the Adsorbed SP Layer by Ellipsometer. Silicon wafers were modified to become hydrophobic and adsorbed SP proteins under the same condition as the preparation of the SP-functionalized silica slides as introduced above. After that, the thickness of the adsorbed SP layer on the Si surfaces in the dry state was measured in the ambient environment by an ellipsometer (SC600 Discrete Wavelength, Shanghai Sanco Instru., China) at the angle of 70° and wavelength of 632.8 nm. The measured phase difference and polarized amplitude component were used to calculate the film thickness. The thickness of the SiO_2 layer on the silicon wafer was 0.58 nm. Then the Cauchy model was used for obtaining the hydrophobic functionalized surfaces and the adsorbed films of SP (assuming the refractive indexes for the hydrophobic layer and SP layer were fixed at 1.40 and 1.45, respectively). The data from six points of the samples were averaged.

Zeta-Potential Measurement. The electrophoretic mobility (μ_E) of the protein (ConA, BSA, LYZ) adsorbed PS latexes and the SP-functionalized silica particles in aqueous solutions were measured with a commercial zeta-potential spectrometer (ZetaPlus, Brookhaven). Following the Smoluchowski equation ($\kappa R \gg 1$), the zeta potential ($\zeta_{potential}$) can be calculated from μ_E as

$$\zeta_{potential} = \frac{\mu_E \eta}{\varepsilon} \quad (1)$$

where η is the viscosity and ε is the dielectric constant of the solvent. Note that silica particles we used in this work have an average diameter of 5 μm; therefore, the adsorption configuration of SP (∼2 nm) to these spherical particles can be considered analogous to the adsorption onto flat glass slide used in TIRM measurements. The mobility of these PS particles (bare, adsorbed with ConA, BSA, and LYZ) and silica particles adsorbed with SP in salty aqueous solution was obtained by taking the average of five individual runs.

Total Internal Reflection Microscope (TIRM) Measurements. The principle of TIRM instrument has been described in previous literature.[20] TIRM is a technique for the direct measurements of interaction energy between a colloid and a flat surface. In a TIRM measurement, an evanescent wave, which decays exponentially with the distance from the interface, is generated at the glass−water surface by a total internal reflection. When a micron-sized probe sphere approaches the surface close enough to enter the evanescent field, the sphere will scatter the evanescent wave. The scattered intensity (I) of the colloidal sphere has been shown to be proportional to that of the evanescent wave and can be written as[20,23,24]

$$I(h) = I_{h\to 0} \exp(-\beta h) \quad (2)$$

DOI: 10.1021/acs.langmuir.5b00090
Langmuir 2015, 31, 3101−3107

where h is the separation distance between the colloidal sphere and the glass surface, β^{-1} is the characteristic penetration length, and $I_{h\to 0}$ is the immobilized particle intensity which can be obtained by depositing the colloidal sphere on the bottom surface with a salty solution (i.e., 100 mM NaCl). Measuring $I(h)$ over time provides a sensitive and nonintrusive method to determine the distance h between the sphere and the bottom surface. After thermal equilibrium, the probable distribution of finding the particle at a certain distance to the wall, $p(h)$, is given by the Boltzmann distribution

$$p(h) = A \exp\left[-\frac{\phi(h)}{k_B T}\right] \tag{3}$$

where A is a constant normalizing the integrated distribution to unity and $\phi(h)$ is the interaction energy potential from the measured intensity. Generally, the interaction potential energy between a charged colloidal particle and a charged surface in aqueous solution is dominated by gravity and the electrostatic interaction between the two surfaces, while van der Waals forces can be neglected since the particle is far away from the bottom surface. In this case, the potential energy between the particle and surface can be described as[20]

$$\phi(h) = B \exp[-\kappa h] + Gh \tag{4}$$

Here B is a function of the surface potential between the bottom and the particle, κ^{-1} is the Debye length, and the effective weight, G, of the particle

$$G = \frac{4}{3}\pi a^3(\rho_p - \rho_s)g \tag{5}$$

where a is the radius of the particle and ρ_p and ρ_s are the densities of the particle and the solution, respectively. Furthermore, eq 4 has a minimum at a separation distance h_m, given by

$$\kappa h_m = \ln\frac{\kappa B}{G} \tag{6}$$

Eliminating B by eq 6, eq 4 can be expressed as

$$\frac{\phi(h) - \phi(h_m)}{kT} = \frac{G}{\kappa kT}\{\exp[-\kappa(h - h_m)] + \kappa(h - h_m) - 1\} \tag{7}$$

In the TIRM measurements, different types of protein-adsorbed PS particles dispersed in solutions with a specific pH value were injected into a sample cell. After setting up, a protein-functionalized PS particle of average brightness was selected, and the interaction potentials between the PS particle and SP-functionalized glass slide in solutions with different pH values were monitored. The protein-adsorbed PS probe particle (diameter = 5.6 μm) dispersed in solutions with total ionic concentration of 0.1 mM from high to low pH values were injected in turn into a sealed sample cell, while the bottom kept using the same SP-functionalized slide. The conductivity of the sample solutions was monitored by a conductivity meter (Cond. Meter 470, Jenway, UK), and the pH value of the sample solution was recorded by the pH meter (pH/mV Meter UB-10, Ultra Basic). All TIRM experiments were performed at room temperature.

RESULTS AND DISCUSSION

Characterization of the Protein-Adsorbed Surfaces. A number of works[25,26] have been conducted to examine the structure and properties of proteins when they are adsorbed to surfaces. Protein adsorption is a very complex process and multiple interactions including hydrophobic interaction, electrostatic interaction, hydrogen bonding, and van der Waals interaction are involved to control the adsorption process. While hydrophobic interaction has been shown to play an important role,[27] other factors such as ionic strength, pH, and bulk concentration can also affect the adsorption process.[28] Note that the isoelectric point (iep) of most proteins in nature is around pH 5.0. We chose two proteins: ConA (iep = 4.5−5.1)[29] and BSA (iep = 4.6−5.4)[30,31] whose iep values are close to pH 5.0. Besides, protein LYZ with a iep of 11.0[32] was also selected in this work for a comparative study.

Table 1 shows the hydrodynamic radius ($\langle R_h \rangle$) of PS particles (diameter = 100 nm) after adsorption of the three kinds of proteins (ConA/BSA/LYZ), together with the reported size of these proteins in bulk. In all cases, $\langle R_h \rangle$ of PS particles increases, indicating that all the surfaces of the PS particles were covered by the three proteins. For ConA and BSA cases, the increased thickness is around 9.5 and 7.9 nm, respectively, which are comparable to the diameter of single protein molecule. Likely, the PS surfaces were coated by a single layer of the proteins if there are not many changes of the conformation of protein during adsorption.[33] However, the situation for LYZ is quite different: the change of $\langle R_h \rangle$ is greater than 12 nm, much larger than the size of a single LYZ, indicating that more than one layer of LYZ may be adsorbed to the PS surface.

Table 1. Hydrodynamic Radius ($\langle R_h \rangle$) and Polydispersity Index (PDI) of Bare PS Particles, Three Kinds of Protein-Functionalized PS Particles (ConA-PS, BSA-PS, LYZ-PS), and Dimensions of These Proteins Obtained from the Literature

	$\langle R_h \rangle$/nm	PDI	dimension of protein/nm
bare PS	50.0	0.117	
ConA-PS	59.5	0.178	$7 \times 7 \times 6$[34]
BSA-PS	57.9	0.177	$9 \times 5.5 \times 5.5$[35]
LYZ-PS	62.4	0.183	$4 \times 3 \times 3$[36]

Table 2 shows the dry state thickness measured by ellipsometer for the hydrophobic modified and SP-functionalized glass slides. After treating with dichlorodimethylsilane, a ~3.23 nm hydrophobic layer has formed, and the contact angle of the clean slide changes from ~2.0° to 96.7°. After immersing in SP solution for at least 12 h and continuously rinsing with DI water, the thickness variation shows that a thin film of SP has been formed on the slide surface, mostly via hydrophobic interaction.

Table 2. Thickness in Dry State Measured by the Ellipsometer of Dichlorodimethylsilane Functionalized and SP Layer on Glass Slides

	hydrophobic layer	SP layer
thickness (nm)	3.23 ± 0.20	2.12 ± 0.19

Besides, the electrostatic properties of the protein-functionalized surfaces were investigated. Figure 1 shows the pH dependence of $\zeta_{potential}$ for SP-functionalized silica particles (SP-silica) in the mixture of NaOH or HCl and 1 mM NaCl at desirable pH values. Note that the $\zeta_{potential}$ of SP-silica measured here will become an important reference for our later TIRM experiments. From Figure 1, the isoelectric point (iep) of SP-silica is ~5.1, slightly different from the value of 4.5 reported before.[37] Norde et al. have divided proteins into two classes, namely "soft" proteins like BSA and "hard" proteins like LYZ.[33] Hard proteins can hardly change its conformation while soft proteins change much easier. It has been shown that SP might belong to the "soft" kind. Actually, SP combines of many globulins with different mass weights, so some kinds of globulins might have a preference to be adsorbed to

DOI: 10.1021/acs.langmuir.5b00090
Langmuir 2015, 31, 3101−3107

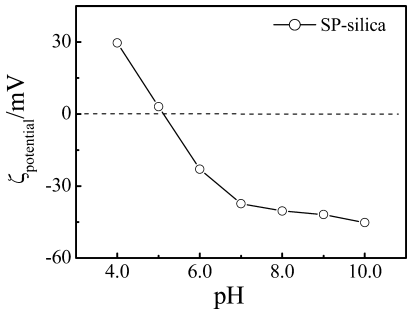

Figure 1. pH dependence of $\zeta_{potential}$ of SP-silica in a mixture of NaOH or HCl with NaCl with similar ionic strength but desirable pH values.

hydrophobic surfaces; besides, the adsorbed SP might adopt different configurations from the bulk ones. Both reasons contribute to the shift of iep. At pH < 5.1, the SP film is positively charged, and $\zeta_{potential}$ decreases with pH sharply; while at pH > 5.1, it is negatively charged, and $\zeta_{potential}$ becomes more negative with increasing pH value. Moreover, we also confirmed that repeated rinsing of the adsorbed-SP layer at different pH value mediums would not cause a significant effect on the properties of the adsorbed SP layers at the glass surfaces.

Interactions between ConA/BSA/LYZ-Functionalized PS and SP-Functionalized Glass Slide (SP-Silica). Figure 2a shows the $\zeta_{potential}$ of the PS particles functionalized with ConA (ConA-PS) and SP-silica. Bare PS particles are always negatively charged at pH > 3.0, and $\zeta_{potential}$ is about −90 mV. It can be seen that after adsorbed with ConA, the $\zeta_{potential}$ of the corresponding PS particles changed greatly compared with bare ones, confirming the existence of the adsorbed protein layers at the particle surface. The iep of ConA-PS is ∼4.5, which is consistent with the reported value of bulk ConA.[29] Figure 2b shows a series of measured potential profiles between the ConA-PS and SP-silica surfaces in medium solution with different pH values but similar ionic concentrations. The medium solution was prepared in the following ways: Typically, for solution at pH = 4.0, it was prepared with 0.1 mM HCl, while solution at pH = 10.0 was prepared with 0.1 mM NaOH. The solution at pH = 7.5 was prepared by mixing 0.1 mM NaCl with quite diluted HCl or NaOH. In this manner, we kept the similar ionic strength for all these solutions, and the difference of the electrostatic interaction induced by the solution medium can be minimized. As can be seen in Figure 2b, interactions between ConA-PS and SP-silica show strong pH dependence. At pH = 7.5−10.0, the two surfaces repulse each other. As pH increases, the distance between the two surfaces (h) increases, indicating the enhanced repulsion between the ConA-PS and SP-silica surfaces. This agrees well with the trend of $\zeta_{potential}$ of the two surfaces which also increases as pH increases.

At this pH range, there are only two force contributions in the measured interaction profiles: electric double-layer repulsion which dominates at the left side of the potential profiles and the gravity which dominates the other side. The fitting of the interaction profiles at pH ranging from 7.0 to 10.0 by eq 4 is shown as the solid line in Figure 2b, and the related parameters are summarized in Table 3. The fitting results show κ^{-1} = 25.9 nm at pH = 7.5 and 26.4 nm at pH 10.0, which are close to the calculated value (∼30 nm) for 0.1 mM NaCl. Meanwhile, the fitted G ∼ 46.2 and 44.7 fN in these two pH values also agree well with the theoretical value (∼45 fN) of PS particles with diameter of ∼5.6 μm. When pH decreases to 5.0, the potential profile is similar to the profile measured at 100

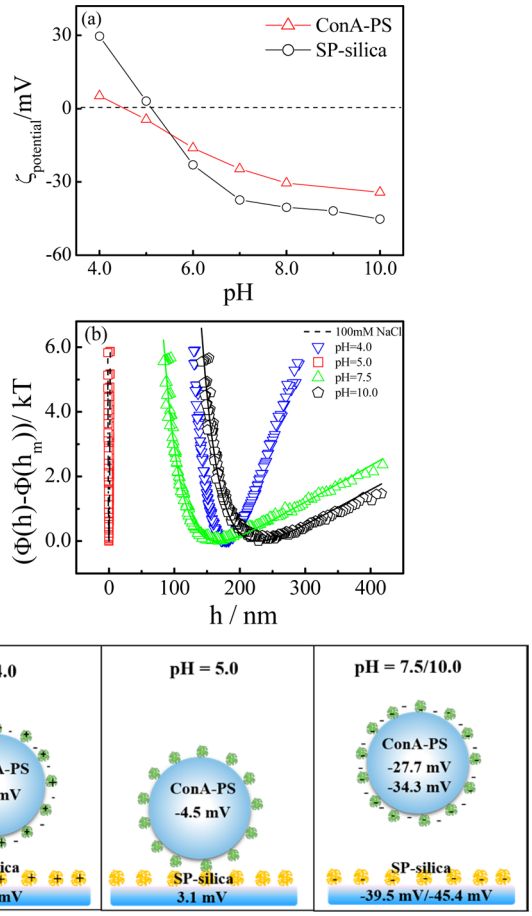

Figure 2. (a) pH-dependent $\zeta_{potential}$ for ConA-PS and SP-silica surface. (b) Potential energy profiles between ConA-PS and SP-silica with pH dependence ranging from 4.0 to 10.0, together with the profile measured at 100 mM NaCl. (c) Schematic of the interactions between ConA-PS and SP-silica surfaces at different pH solutions.

Table 3. Fitted Parameters by Eq 4 and $\zeta_{potential}$ for ConA-PS (ζ_{up}) and SP-Silica (ζ_{down}) for the Potential Energy Profiles in Figure 2b between ConA-PS and SP-Silica Surfaces

pH	G/fN	κ^{-1}/nm	h_m/nm	ζ_{up}/mV	ζ_{down}/mV
4.0			179.2	+5.2	+29.6
5.0			0	−4.5	+3.1
7.5	46.2 ± 1.5	25.9 ± 0.4	167.4	−27.7	−39.5
10.0	44.7 ± 2.2	26.4 ± 0.5	228.5	−34.3	−45.4

mM NaCl solution where ConA-PS has been tightly adhered to the SP-silica bottom surface. This might be due to two reasons: On one hand, the two surfaces are nearly neutral at this pH value shown in Figure 2a; double-layer repulsion between the two surfaces is significantly reduced. On the other hand, the protein-functionalized surfaces exhibit strong hydrophobic properties, enhancing the adhesion of the two surfaces. Zhong et al. have demonstrated that SP exhibits a hydrophobic character at a pH close to its iep.[38] However, it is interesting to note that when pH is further reduced to pH = 4.0, the ConA-PS particles start to move again with a separation distance from the bottom around 179.4 nm. At pH 4.0, SP-silica is positively charged ($\zeta_{potential}$ = 29.6 mV), while the ConA-PS is less positively charged ($\zeta_{potential}$ = 5.2 mV, almost neutral). Note that the bare PS surface is originally highly negatively charged ($\zeta_{potential}$ ∼ −90 mV); due to small size of the ConA, one can

DOI: 10.1021/acs.langmuir.5b00090
Langmuir 2015, 31, 3101−3107

suspect that the adsorbed ConA films are heterogeneous, consisting of individual adsorbed proteins that are unevenly distributed on the negatively charged PS sphere. In this case, when ConA-PS interacts closely with SP-silica surface, a positively charged SP-silica surface might face a negatively charged uncovered PS surface, resulting in a net electrostatic attraction. The two surfaces thereby likely interact with both electrostatic repulsion and attraction as schematically shown in Figure 2c. We note that Silbert et al. reported a long-ranged attraction that can be raised between disordered heterogeneous surfaces.[39] This is similar to our situation. In other words, the protein adsorbed surfaces bear randomly distributed positive and negative charge patches, but which are close to neutral under this pH value as shown in Figure 2c. Positive charge repulsion cannot compensate for negative−positive charge attraction, and as a result, the particle at pH 4 moves restrictedly in a limited range and the measured potential energy profile shows a long-ranged attraction force.

From Figure 3a, we can see that interactions between BSA-adsorbed surfaces also shows similar pH-dependent behavior compared with ConA. Note that the iep of BSA-PS is 4.7, close to the reported value of bulk BSA.[40] The BSA-PS and SP-silica surfaces are expected to carry opposite charges in the range 4.7 < pH < 5.1 and the same charge sign in the rest range. Figure 3b shows a series of potential profiles between the BSA-PS and SP-silica surfaces as a function of pH with similar ionic strength. The experimental procedures were prepared in a similar manner to the interaction measurements between ConA-PS and SP-silica surfaces. The fittings of the interaction potentials from 7.5 to 10.0 by eq 4 are shown as the solid line in Figure 3b, and the related parameters are summarized in Table 4. The

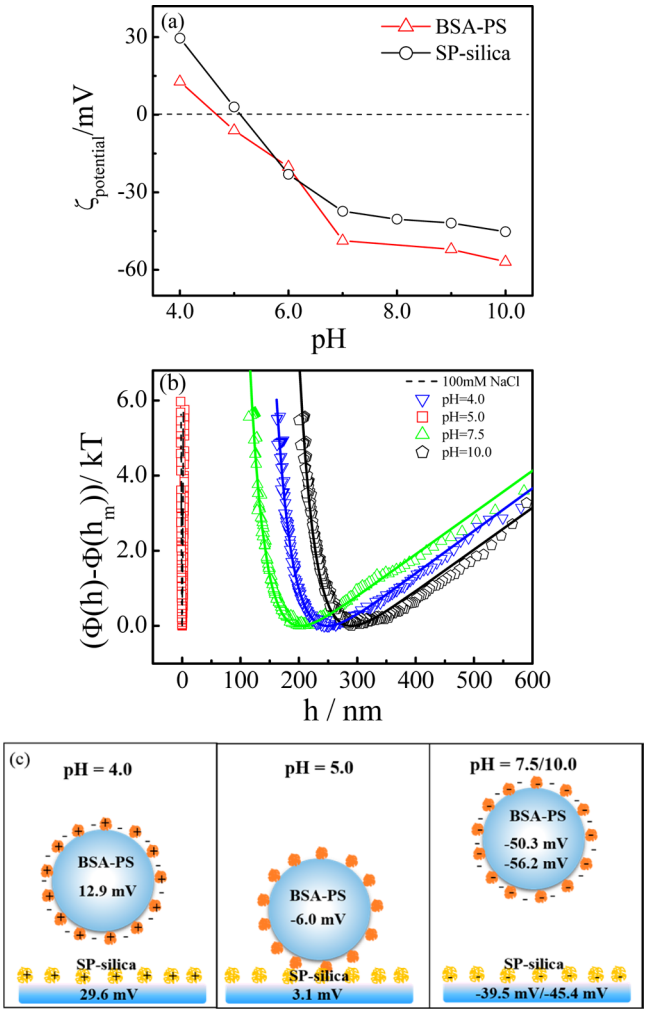

Figure 3. (a) pH-dependent $\zeta_{potential}$ for BSA-PS and SP-silica surface. (b) Potential profiles between BSA-PS and SP-silica surfaces with pH dependence ranging from 4.0 to 10.0, together with the profile measured at 100 mM NaCl. (c) Schematic of the interactions between BSA-PS and SP-silica surfaces at different pH solutions.

Table 4. Fitted Parameters by Eq 4 and $\zeta_{potential}$ for BSA-PS (ζ_{up}) and SP-Silica (ζ_{down}) for the Potential Energy Profiles in Figure 4 between BSA-PS and SP-Silica Surfaces

pH	G/fN	κ^{-1}/nm	h_m/nm	ζ_{up}/mV	ζ_{down}/mV
4.0	46.3 ± 1.0	27.6 ± 0.3	249	+12.9	+29.6
5.0			0	−6.0	+3.1
7.5	45.7 ± 1.1	25.9 ± 0.3	202.8	−50.3	−39.5
10.0	45.3 ± 1.3	26.8 ± 0.3	289.9	−56.2	−45.4

fitting lead to κ^{-1} = 25.9 nm at pH = 7.5 and 26.8 nm at pH 10.0, and both values are close to the calculated value (∼30 nm) for 0.1 mM ionic strength. Besides, the obtained G ∼ 45.7 and 45.3 fN in these two pH values agree well with the theoretical value (∼45 fN), indicating that double layer repulsion dominates at these conditions. When pH is decreased to 5.0, the interactions between BSA-PS and SP-silica exhibit similar trends as ConA-PS and SP-silica; the particles are adhered to the SP-functionalized bottom surface, likely due to the weaken electrostatic repulsion at pH 5.0. In contrast to ConA-PS, at pH = 4.0 the potential energy profile for BSA-PS can be fitted by eq 4 to give κ^{-1} = 27.6 nm and G = 46.3 fN, which are close to the theoretical values, indicating that at this pH value electrostatic repulsion still dominates. The result differs from the ConA-PS series because BSA-PS particles show a higher positive charge. The repulsion induced by such positive charges is much larger than negative−positive charge attraction. The larger electrostatic repulsive force can finally let BSA-PS particles moving freely.

Concerning the adsorption properties of LYZ, the situation is quite different. LYZ is a protein that is positively charged at pH ∼ 7, and it differs from most of the proteins in nature. It was thus selected in our experiments to study the influence of electric properties of the adsorbed proteins to the related interactions between protein-functionalized surfaces. The pH dependence of $\zeta_{potential}$ for LYZ-PS is presented in Figure 4a. It can be seen that LYZ-PS surfaces show a large shift of iep (iep ∼ 5.7) compared with the LYZ bulk solution where the iep of bulk LYZ is given as ∼11.0.

Figure 4b shows a series of potential profiles between the LYZ-PS and SP-silica surfaces as a function of pH with similar ionic strength for the interaction measurements between ConA-PS/BSA-PS and SP-silica surfaces. Results from the energy profiles measured by TIRM agree well with the $\zeta_{potential}$ data. At pH = 7.5−10.0, LYZ is positively charged while PS is highly negatively charged. However, negative charge repulsion is much larger than positive−negative charge attraction. So repulsion still domains under these conditions, and the potential energies also fit well with eq 4. The fitted results are κ^{-1} = 28.0 nm, G = 45.0 fN for pH = 7.5 and κ^{-1} = 28.0 nm, G = 47.1 fN for pH 10.0, which are close to the calculated values (κ^{-1} ∼ 30 nm and G ∼ 45 fN). Also when pH = 5.0, all

DOI: 10.1021/acs.langmuir.5b00090
Langmuir 2015, 31, 3101−3107

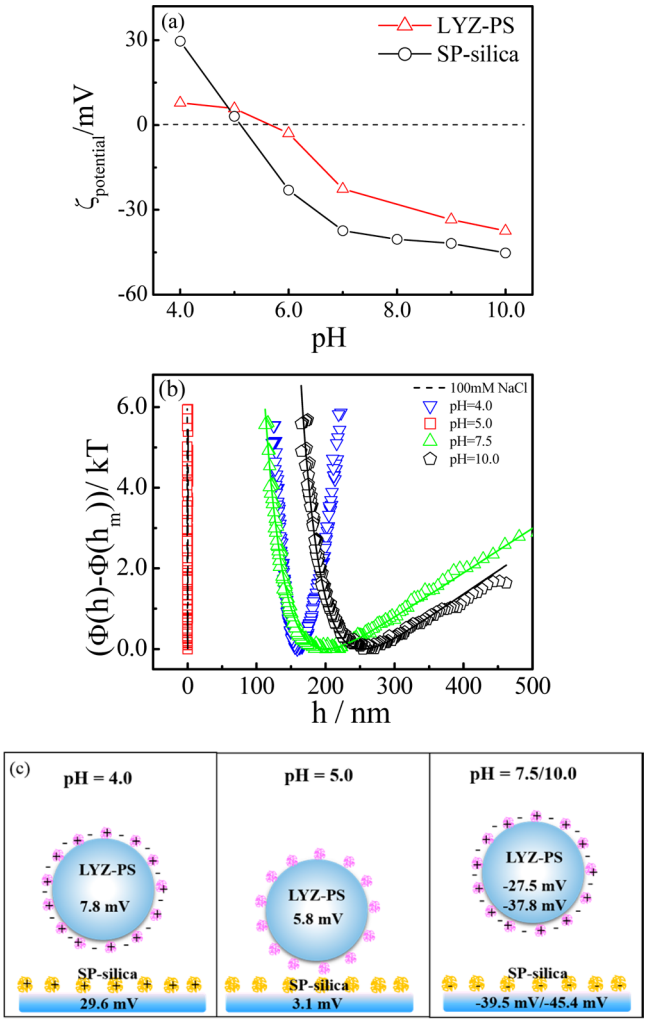

Figure 4. (a) pH-dependent $\zeta_{potential}$ for LYZ-PS and SP-silica surface. (b) Potential profiles between LYZ-PS and SP-silica surfaces with pH dependence ranging from 4.0 to 10.0, together with the profile measured at 100 mM NaCl solution. (c) Schematic of the interactions between LYZ-PS and SP-silica surfaces at different pH solutions.

the particles are attached to the surface, and the surface hydrophobicity plays an important role in their interactions. At pH = 4.0, LYZ-adsorbed surfaces bear randomly distributed positive and negative charge patches, and the overall charges are close to neutral under this pH value. The particles at this pH value move restrictedly, and the potential energy curve shows a strong attraction force, which is similar to the ConA-PS particles.

Comparing these three protein-adsorbed systems, we can see that all the TIRM results agree well with the $\zeta_{potential}$ data. At pH 7.5−10.0, all these three protein-functionalized particles move freely above the SP-functionalized surface and double-layer repulsion domains for the long-range interaction. At pH = 5.0, all these three protein-functionalized particles are adhered to the surface. This can be related to the lessened electric repulsion and enhanced hydrophobic forces involved in the short-range interactions. However, at pH = 4.0, only the highly charged BSA-PS can move freely due to the strong double-layer repulsion, while ConA-PS and LYZ-PS particles move restrictively which might be linked to the randomly distributed positive and negative charge patches on the surface. We can conclude that the electrostatic properties of protein-functionalized PS surfaces are determined by not only the protein properties but also the uncovered surfaces of PS particles. In addition, double-layer repulsion is an important long-ranged interaction contributing to the interactions between protein-functionalized surfaces.

Table 5. Fitted Parameters by Eq 4 and $\zeta_{potential}$ for LYZ-PS (ζ_{up}) and SP-Silica (ζ_{down}) for the Potential Energy Profiles in Figure 4 between LYZ-PS and SP-Silica Surface

pH	G/fN	κ^{-1}/nm	h_m/nm	ζ_{up}/mV	ζ_{down}/mV
4.0			159.0	+7.8	+29.6
5.0			0	+5.8	+3.1
7.5	45.0 ± 0.8	28.0 ± 0.2	200.6	−27.5	−39.5
10.0	47.1 ± 1.8	28.0 ± 0.5	254	−37.8	−45.4

CONCLUSION

TIRM was introduced as an invasive approach to study the interactions between several kinds of protein adsorbed surfaces under Brownian motion. Combining with zeta potential and thickness measurements, we found that the iep of the protein-functionalized surfaces shifted from the bulk protein solutions in different extents. At pH close to iep, adhesion was found between two protein-adsorbed surfaces. They can be related to the reduced double-layer repulsion and strong hydrophobic attractions between the adsorbed protein films when the protein-functionalized surfaces become neutral. However, at pH far beyond the iep of the two protein-functionalized surfaces, one of the surfaces that adsorbed with the SP can resist to the surface adsorbed with either ConA, BSA, or LYZ proteins due to the strong electrostatic repulsion, and the corresponding potential energy curves fitted well with the classic DLVO theory. This study provides an insight into the mechanism of the protein resistance and the interactions involved in protein-functionalized surfaces.

AUTHOR INFORMATION

Corresponding Authors

*E-mail tongai@cuhk.edu.hk (T.N.).
*E-mail msxjgong@scut.edu.cn (X.G.).

Notes

The authors declare no competing financial interest.

ACKNOWLEDGMENTS

The financial support of this work by the Hong Kong Special Administration Region (HKSAR) General Research Fund (CUHK402712, 2130304) and the National Natural Science Foundation of China (21404044) is gratefully acknowledged.

REFERENCES

(1) Yuan, L.; Yu, Q.; Li, D.; Chen, H. Surface modification to control protein/surface interactions. *Macromol. Biosci.* **2011**, *11* (8), 1031−1040.

(2) Nel, A. E.; Madler, L.; Velegol, D.; Xia, T.; Hoek, E. M. V.; Somasundaran, P.; Klaessig, F.; Castranova, V.; Thompson, M. Understanding biophysicochemical interactions at the nano-bio interface. *Nat. Mater.* **2009**, *8* (7), 543−557.

(3) Ma, C.; Wu, B.; Zhang, G. Protein−protein resistance investigated by quartz crystal microbalance. *Colloids Surf., B* **2013**, *104*, 5−10.

DOI: 10.1021/acs.langmuir.5b00090
Langmuir 2015, 31, 3101−3107

(4) Bosker, W. T. E.; Iakovlev, P. A.; Norde, W.; Cohen Stuart, M. A. BSA adsorption on bimodal PEO brushes. *J. Colloid Interface Sci.* **2005**, *286* (2), 496−503.
(5) White, A. D.; Nowinski, A. K.; Huang, W.; Keefe, A. J.; Sun, F.; Jiang, S. Decoding nonspecific interactions from nature. *Chem. Sci.* **2012**, *3* (12), 3488.
(6) Yu, Q.; Zhang, Y.; Wang, H.; Brash, J.; Chen, H. Anti-fouling bioactive surfaces. *Acta Biomater.* **2011**, *7* (4), 1550−1557.
(7) McArthur, S. L.; McLean, K. M.; Kingshott, P.; St John, H. A. W.; Chatelier, R. C.; Griesser, H. J. Effect of polysaccharide structure on protein adsorption. *Colloids Surf., B* **2000**, *17* (1), 37−48.
(8) Johnell, M.; Larsson, R.; Siegbahn, A. The influence of different heparin surface concentrations and antithrombin-binding capacity on inflammation and coagulation. *Biomaterials* **2005**, *26* (14), 1731−1739.
(9) Ruiz, L.; Hilborn, J. G.; Leonard, D.; Mathieu, H. J. Synthesis, structure and surface dynamics of phosphorylcholine functional biomimicking polymers. *Biomaterials* **1998**, *19* (11-12), 987−998.
(10) Hadidi, M.; Zydney, A. L. Fouling behavior of zwitterionic membranes: Impact of electrostatic and hydrophobic interactions. *J. Membr. Sci.* **2014**, *452*, 97−103.
(11) Chien, H.-W.; Tsai, C.-C.; Tsai, W.-B.; Wang, M.-J.; Kuo, W.-H.; Wei, T.-C.; Huang, S.-T. Surface conjugation of zwitterionic polymers to inhibit cell adhesion and protein adsorption. *Colloids Surf., B* **2013**, *107*, 152−159.
(12) Kingshott, P.; Thissen, H.; Griesser, H. J. Effects of cloud-point grafting, chain length, and density of PEG layers on competitive adsorption of ocular proteins. *Biomaterials* **2002**, *23* (9), 2043−2056.
(13) Zhang, M. Q.; Desai, T.; Ferrari, M. Proteins and cells on PEG immobilized silicon surfaces. *Biomaterials* **1998**, *19* (10), 953−960.
(14) Pillai, S.; Arpanaei, A.; Meyer, R. L.; Birkedal, V.; Gram, L.; Besenbacher, F.; Kingshott, P. Preventing protein adsorption from a range of surfaces using an aqueous fish protein extract. *Biomacromolecules* **2009**, *10* (10), 2759−2766.
(15) Wang, Z.; Lienemann, M.; Qiau, M.; Linder, M. B. Mechanisms of protein adhesion on surface films of hydrophobin. *Langmuir* **2010**, *26* (11), 8491−8496.
(16) Everett, W. N.; Wu, H.-J.; Anekal, S. G.; Sue, H.-J.; Bevan, M. A. Diffusing colloidal probes of protein and synthetic macromolecule interactions. *Biophys. J.* **2007**, *92* (3), 1005−1013.
(17) Eichmann, S. L.; Meric, G.; Swavola, J. C.; Bevan, M. A. Diffusing colloidal probes of protein−carbohydrate interactions. *Langmuir* **2013**, *29* (7), 2299−2310.
(18) Everett, W. N.; Bevan, M. A. kT-Scale interactions between supported lipid bilayers. *Soft Matter* **2014**, *10* (2), 332.
(19) Guerrero, P.; Stefani, P. M.; Ruseckaite, R. A.; de la Caba, K. Functional properties of films based on soy protein isolate and gelatin processed by compression molding. *J. Food Eng.* **2011**, *105* (1), 65−72.
(20) Prieve, D. C. Measurement of colloidal forces with TIRM. *Adv. Colloid Interface Sci.* **1999**, *82* (1-3), 93−125.
(21) Everett, W. N.; Beltran-Villegas, D. J.; Bevan, M. A. Concentrated diffusing colloidal probes of Ca^{2+}-dependent cadherin interactions. *Langmuir* **2010**, *26* (24), 18976−18984.
(22) Bratek-Skicki, A.; Żeliszewska, P.; Adamczyk, Z. Tuning conformations of fibrinogen monolayers on latex particles by pH of adsorption. *Colloids Surf., B* **2013**, *103*, 482−488.
(23) Bevan, M. A.; Prieve, D. C. Direct measurement of retarded van der Waals attraction. *Langmuir* **1999**, *15* (23), 7925−7936.
(24) Biggs, S.; Dagastine, R. R.; Prieve, D. C. Oscillatory packing and depletion of polyelectrolyte molecules at an oxide-water interface. *J. Phys. Chem. B* **2002**, *106* (44), 11557−11564.
(25) Kochwa, S.; Brownell, M.; Rosenfie, Re; Wasserma, Lr. Adsorption of proteins by polystyrene particles. I. Molecular unfolding and acquired immunogenicity of IGG. *J. Immunol* **1967**, *99* (5), 981.
(26) Galisteo, F.; Norde, W. Adsorption of lysozyme and alpha-lactalbumin on poly(styrenesulphonate) latices. 2. Proton titrations. *Colloids Surf., B* **1995**, *4* (6), 389−400.
(27) Kim, J.-H.; Yoon, J.-Y. Protein adsorption on polymer particles. In *Encyclopedia of Surface and Colloid Science*; Hubbard, A. T., Ed.; Marcel Dekker, Inc.: New York, 2002; Vol. *1*, p 4373.
(28) Adamczyk, Z.; Bratek-Skicki, A.; Dąbrowska, P.; Nattich-Rak, M. Mechanisms of fibrinogen adsorption on latex particles determined by zeta potential and AFM measurements. *Langmuir* **2012**, *28* (1), 474−485.
(29) Oh, E.; Lee, D.; Kim, Y.-P.; Cha, S. Y.; Oh, D.-B.; Kang, H. A.; Kim, J.; Kim, H.-S. Nanoparticle-based energy transfer for rapid and simple detection of protein glycosylation. *Angew. Chem.* **2006**, *118* (47), 8127−8131.
(30) Brewer, S. H.; Glomm, W. R.; Johnson, M. C.; Knag, M. K.; Franzen, S. Probing BSA binding to citrate-coated gold nanoparticles and surfaces. *Langmuir* **2005**, *21* (20), 9303−9307.
(31) Shi, Q. S.; Zhou, Y.; Sun, Y. Influence of pH and ionic strength on the steric mass-action model parameters around the isoelectric point of protein. *Biotechnol. Prog.* **2005**, *21* (2), 516−523.
(32) Seeber, S. J.; White, J. L.; Hem, S. L. Predicting the adsorption of proteins by aluminum-containing adjuvants. *Vaccine* **1991**, *9* (3), 201−203.
(33) Norde, W. My voyage of discovery to proteins in flatland···and beyond. *Colloids Surf., B* **2008**, *61* (1), 1−9.
(34) Waner, M. J.; Gilchrist, M.; Schindler, M.; Dantus, M. Imaging the molecular dimensions and oligomerization of proteins at liquid/solid interfaces. *J. Phys. Chem. B* **1998**, *102* (9), 1649−1657.
(35) Kaufman, E. D.; Belyea, J.; Johnson, M. C.; Nicholson, Z. M.; Ricks, J. L.; Shah, P. K.; Bayless, M.; Pettersson, T.; Feldoto, Z.; Blomberg, E.; Claesson, P.; Franzen, S. Probing protein adsorption onto mercaptoundecanoic acid stabilized gold nanoparticles and surfaces by quartz crystal microbalance and zeta-potential measurements. *Langmuir* **2007**, *23* (11), 6053−6062.
(36) Jachimska, B.; Kozłowska, A.; Pajor-Świerzy, A. Protonation of lysozymes and its consequences for the adsorption onto a mica surface. *Langmuir* **2012**, *28* (31), 11502−11510.
(37) Klish, W. J.; Baker, S. S.; Cochran, W. J.; Flores, C. A.; Georgieff, M. K.; Jacobson, M. S.; Lake, A. M.; Blum, D.; Harris, S. S.; Hubbard, V. S.; Levin, E.; Prendergast, A.; Smith, A. E.; Yetley, E.; Zlotkin, S.; Lauer, R. M. Soy protein-based formulas: Recommendations for use in infant feeding. *Pediatrics* **1998**, *101* (1), 148−153.
(38) Zhong, Z.; Sun, X. S.; Wang, D. Isoelectric pH of polyamide−epichlorohydrin modified soy protein improved water resistance and adhesion properties. *J. Appl. Polym. Sci.* **2007**, *103* (4), 2261−2270.
(39) Silbert, G.; Ben-Yaakov, D.; Dror, Y.; Perkin, S.; Kampf, N.; Klein, J. Long-ranged attraction between disordered heterogeneous surfaces. *Phys. Rev. Lett.* **2012**, *109* (16).
(40) Shouren, G.; Kojio, K.; Takahara, A.; Kajiyama, T. Bovine serum albumin adsorption onto immobilized organotrichlorosilane surface: Influence of the phase separation on protein adsorption patterns. *J. Biomater. Sci., Polym. Ed.* **1998**, *9* (2), 131−150.

DOI: 10.1021/acs.langmuir.5b00090
Langmuir 2015, 31, 3101−3107